

Swapped Entanglement in High-Dimensional Quantum Systems

S. M. Zangi¹, Chitra Shukla^{2,*}, Khalid Naseer,¹ and Saeed Haddadi^{3,†}

¹*Department of Physics, University of Sargodha, Sargodha 40100, Pakistan*

²*Interdisciplinary Centre for Security, Reliability and Trust (SnT), University of Luxembourg 1855, Luxembourg*

³*School of Particles and Accelerators, Institute for Research in Fundamental Sciences (IPM), P.O. Box 19395-5531, Tehran, Iran*

Entanglement swapping is a fundamental protocol in quantum information processing that enables the distribution of entanglement between distant quantum systems. In this work, we first extend the concept of entanglement swapping to higher-dimensional quantum systems, specifically qudits. We then analyze the dynamics of entanglement swapping and quantify the average swapped entanglement in terms of concurrence and negativity. Our results demonstrate that higher-dimensional systems offer enhanced entanglement distribution capabilities compared to qubit-based protocols. We also discuss the application of entangled qudits in terms of long-distance teleportation that provides the base for quantum repeaters. Furthermore, we discuss the entanglement swapping for a real and noisy system. The behaviors of entanglement against fidelity with different dimensions are also discussed.

I. INTRODUCTION

Quantum entanglement is a distinct feature of quantum mechanics, where two or more particles become interconnected regardless of the distance that separates them [1]. This peculiar connection arises when particles interact in specific ways, and their quantum state cannot be described independently for each particle. Entanglement forms the foundation of many cutting-edge advancements in quantum science, including quantum teleportation [2], quantum key distribution [3], super-dense coding [4], quantum secret sharing [5] and quantum secure direct communication [6], etc. This phenomenon also defies classical intuitions about locality and separability, as changes to one particle's state instantly influence its entangled partner [7]. A particularly fascinating extension of this concept is entanglement swapping [8, 9], which demonstrates how entanglement can be transferred between particles that have never interacted directly.

Entanglement swapping is an advanced quantum process that creates correlations between particles that were initially unentangled and independent [10, 11]. This is achieved by preparing two pairs of entangled particles, such as A-B and C-D, and then performing a Bell-state measurement on one particle from each pair, such as B and C. This measurement projects the remaining particles, A and D, into an entangled state, even though they have never interacted directly. This process is illustrated in Fig. 1.

Entanglement swapping is crucial for extending the range of quantum entanglement, making it a cornerstone of quantum communication networks [12]. The linking of entangled segments facilitates the development of quantum repeaters [13]. These repeaters are essential

for achieving long-distance quantum communication and building scalable quantum internet infrastructure [14].

This work investigates the phenomenon of entanglement swapping in qudit systems, emphasizing its implications for quantum networks and high-dimensional quantum communication. Building upon foundational knowledge of entanglement quantifiers such as concurrence and negativity, the study explores the intricate relationships between these measures and fidelity across varying dimensions. It highlights the enhanced efficiency of entanglement swapping in higher dimensions due to the increased degrees of freedom. Furthermore, practical scenarios involving noisy quantum systems are addressed, showcasing methods to maintain and optimize entanglement through techniques like isotropic state analysis. The results advance our understanding of entanglement dynamics in complex quantum systems, offering valuable insights for applications in quantum repeaters and teleportation protocols.

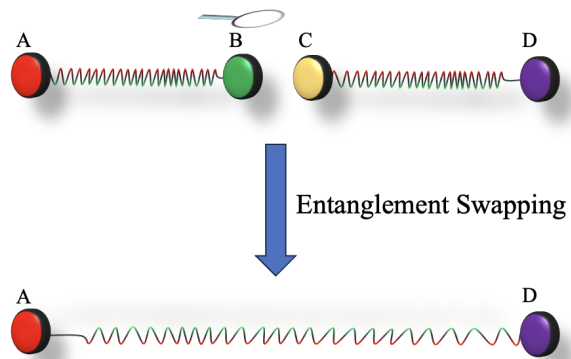


FIG. 1. The top part of the figure illustrates two independent entangled pairs: (A, B) and (C, D). A Bell-state measurement is performed on particles B and C, leading to entanglement swapping. As a result, unentangled particles A and D become entangled in the bottom part of the figure.

* chitra.shukla@uni.lu

† haddadi@ipm.ir

A growing amount of research indicates that certain techniques are required for the purification and entanglement swapping of quantum systems. Due to the relative sensitivity of the operation and quantum systems, even minor modifications can result in significant changes to the output state. Entanglement swapping of starting states into maximally entangled states is discussed by a number of earlier investigations [8–11]. This study on qudit entanglement swapping builds upon and extends prior research on entanglement dynamics and swapping mechanisms in both qubit and qudit systems.

Although foundational works [11, 15–17] explored the dynamics of entanglement swapping by focusing on simple relationships and multi-swap scenarios, our paper ventures into the high-dimensional realm of qudits and the quantification of entanglement of final states. Similarly, the study on dissipative systems by Nourmandipour and Tavassoly [18] delved into the effects of non-Markovian environments and detuning in qubit-based entanglement swapping. The numerical study of entanglement purification via entanglement swapping among qubits-based systems has been studied in Ref. [19]. It establishes a formal upper bound on the achievable output concurrence and demonstrates how optimal entanglement purification can be attained. In contrast, our work focuses on the practical advantages and challenges of qudits-based systems. We discuss their enhanced capacity for high-dimensional entanglement and resilience to noise, analyzed through measures like I-concurrence [20] and negativity [21]. By bridging the gap between foundational qubit studies and the complexities of high-dimensional qudits, this paper provides new insights into the potential of qudits for robust and efficient quantum communication and network protocols.

The article is organized as follows. Section II describes the entanglement swapping among pure qudit systems in detail and the application of the swapped entanglement. Section III demonstrates entanglement swapping for noisy qudit systems. The final section IV contains the concluding remarks.

II. ENTANGLEMENT SWAPPING AMONG QUDIT SYSTEMS

With the realization of high-dimensional quantum states [22], it is of practical importance to study the entanglement swapping among qudit systems. Suppose there are two d -level bipartite pure systems that belong to Hilber spaces $\mathcal{H}_A \otimes \mathcal{H}_B$ and $\mathcal{H}_C \otimes \mathcal{H}_D$, respectively. In the Schmidt form, one can write these states as follows

$$\begin{aligned} |\phi\rangle_{AB} &= \sum_{j_1=0}^{d-1} \sqrt{p_{j_1}} |j_1 j_1\rangle_{AB}, \\ |\phi\rangle_{CD} &= \sum_{j_2=0}^{d-1} \sqrt{p'_{j_2}} |j_2 j_2\rangle_{CD}, \end{aligned} \quad (1)$$

where $\sum_{j_1=0}^{d-1} p_{j_1} = \sum_{j_2=0}^{d-1} p'_{j_2} = 1$. Let the dimension of $\mathcal{H}_A \otimes \mathcal{H}_B$ is finite, therefore, we can quantify the entanglement of $|\phi\rangle_{AB}$ by the method developed by Rungta *et al.* [20] in terms of I-concurrence as

$$C(|\phi\rangle_{AB}) = \sqrt{2[1 - \text{tr}(\rho_A^2)]} = \sqrt{2[1 - \text{tr}(\rho_B^2)]}. \quad (2)$$

Also, the negativity [23] of the biqudit state $|\phi\rangle_{AB}$ can be obtained as

$$\mathcal{N}(|\phi\rangle_{AB}) = \frac{2}{d-1} \sum_{i_1 < j_1} \sqrt{p_{i_1} p_{j_1}}. \quad (3)$$

Similarly, one can calculate the I-concurrence and negativity for the state $|\phi\rangle_{CD}$.

The initial state of our four-qudit system is

$$|\Phi\rangle_{ABCD} = \sum_{j_1, j_2=0}^{d-1} \sqrt{p_{j_1} p'_{j_2}} |j_1 j_1 j_2 j_2\rangle_{ABCD}. \quad (4)$$

Performing a Bell measurement on the particles (B, C), one gets

$$|\Psi_{uv}\rangle_{BC} = \frac{1}{\sqrt{d}} \sum_{l=0}^{d-1} e^{\frac{2\pi i}{d} lu} |l\rangle_B |l \oplus v\rangle_C, \quad (5)$$

where $u, v \in \{0, 1, \dots, d-1\}$ and \oplus denotes modulo d addition. Then, the unentangled particles A and D are projected onto an entangled state

$$|\Phi_{uv}\rangle_{AD} = \frac{1}{\sqrt{P_{uv}}} \sum_{l=0}^{d-1} \sqrt{p_l p'_{l \oplus v}} e^{\frac{-2\pi i}{d} lu} |l\rangle_A |l \oplus v\rangle_D, \quad (6)$$

where normalization factor is $P_{uv} = \sum_{l=0}^{d-1} p_l p'_{l \oplus v}$. The probability of any outcome state $|\Psi_{uv}\rangle_{BC}$ is P_{uv}/d . The probabilities of the outcome quantum state and the final entangled state depend on the initial four-qudit state. The probabilities of either state can be calculated by taking the inner product of the joint state $|\Phi\rangle_{ABCD}$ with the desired state.

The I-concurrence of the state $|\Phi_{uv}\rangle_{AD}$ is derived by

$$C_I(|\Phi_{uv}\rangle_{AD}) = \left[2 \left(1 - \frac{1}{(P_{uv})^2} \sum_{l=0}^{d-1} (p_l p'_{l \oplus v})^2 \right) \right]^{1/2}. \quad (7)$$

The average I-concurrence can be obtained by multiplying the above expression with the probability P_{uv}/d and adding the results for all possible outcomes, namely

$$C_I^{(\text{av})} = \sqrt{2} \sum_{v=0}^{d-1} \left[\left(\sum_{l=0}^{d-1} p_l p'_{l \oplus v} \right)^2 - \sum_{l=0}^{d-1} (p_l p'_{l \oplus v})^2 \right]^{1/2}. \quad (8)$$

This measure quantifies entanglement based on the square root of a sum of terms involving the probabilities p_l and $p'_{l \oplus v}$, where l or v ranges from 0 to $d-1$. The

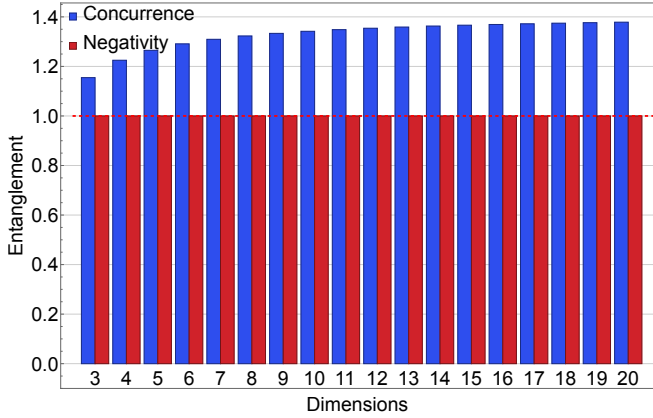


FIG. 2. (Color Online) This plot illustrates the average entanglement of the final states of particles AD, which is generated following entanglement swapping, quantified in terms of I-concurrence and negativity.

presence of nonzero values of $C_I^{(\text{av})}$ indicates the generation of entanglement between particles A and D.

The negativity of the state $|\Phi_{uv}\rangle_{AD}$ is

$$\mathcal{N}(|\Phi_{uv}\rangle_{AD}) = \frac{2}{P_{uv}(d-1)} \sum_{i < j} \sqrt{p_i p'_{i \oplus v} p_j p'_{j \oplus v}}. \quad (9)$$

Note that the phase factor $e^{-\frac{2\pi i}{d} lu}$ disappears in I-concurrence and negativity expressions because it cancels out in the density matrix $|\Phi_{uv}\rangle_{AD} \langle \Phi_{uv}|$. So, the negativity depends only on v and we can write $\mathcal{N}(|\Phi_{uv}\rangle_{AD})$ as \mathcal{N}_v . Since there are d^2 possible Bell measurements on particles A and D, the total number of possible entangled states after swapping is also d^2 . The average negativity of d^2 possible final states $|\Phi_{uv}\rangle_{AD}$ after entanglement swapping can be calculated by

$$\mathcal{N}_{\text{av}} = \sum_{u,v=0}^{d-1} \frac{P_{uv}}{d} \mathcal{N}_v = \frac{2}{(d-1)} \sum_{v=0}^{d-1} \sum_{i < j} \sqrt{p_i p'_{i \oplus v} p_j p'_{j \oplus v}}. \quad (10)$$

If the value of I-concurrence becomes zero, then entanglement is not present between particles; otherwise, particles are entangled. However, this is true for negativity under certain conditions [24].

The initial probabilities (p_j and p'_j) of the Schmidt decomposed states influence the final entanglement between A and D. The specific distribution of these probabilities can lead to varying degrees of entanglement. The success of entanglement swapping also relies on a successful Bell state measurement on particles B and C. The outcome of this measurement determines the specific entangled state shared by A and D.

Maximally entangled states are characterized by having the highest possible degree of correlation between the constituent parts. If we take both AB and CD states

maximally entangled, then we have $p_{j_1} = p'_{j_2} = 1/d$. The entanglement swapping among these states produces maximally entangled states of particles AD.

For this case, the average I-concurrence and average negativity of final states are plotted in Fig. 2. This figure illustrates the behavior of average I-concurrence (blue bars) and negativity (red bars) as a function of dimension d ranging from 3 to 20. The $C_I^{(\text{av})}$ depends on the dimension d but $\mathcal{N}^{(\text{av})}$ remains constant with the change in dimensions. As d increases, $C_I^{(\text{av})}$ also increases, which means the entanglement swapping process is more effective for higher-dimensional systems. This is meaningful because there are more degrees of freedom for entanglement in higher dimensions.

Negativity, being a normalized entanglement measure, is constrained to a maximum value of 1. This makes it an effective tool for comparing entanglement across different dimensions. However, this normalization also imposes a limitation, as it may not fully capture the increasing complexity and strength of entanglement in higher-dimensional quantum systems. On the other hand, I-concurrence is not a normalized measure and exhibits values exceeding 1 as the dimension increases. This behavior indicates that I-concurrence is more sensitive to the enhanced entanglement properties present in high-dimensional systems and provides a more comprehensive characterization of entanglement. The fact that negativity saturates at one suggests that it may underestimate entanglement in larger dimensions, whereas I-concurrence continues to scale and reflects the richer structure of quantum correlations in qudit-based systems. This makes I-concurrence a more effective entanglement measure for higher-dimensional quantum systems because it better captures the increasing entanglement resources available. While negativity remains useful for its simplicity and bounded nature, I-concurrence provides a deeper and more accurate understanding of entanglement dynamics in high-dimensional spaces, making it a superior choice for analyzing entanglement in quantum information science.

The final state $|\Phi_{uv}\rangle_{AD}$ has a wide range of applications; e.g. long-distance teleportation can harness the advantage of qudit Bell entangled based quantum repeaters. Specifically, $|\Phi_{uv}\rangle_{AD}$ can be used as quantum repeaters in a non-terrestrial quantum network application to teleport an unknown qudit system from one end to the other end via several intermediate nodes. Before executing qudit teleportation, it is necessary to perform the purification [25] of $|\Phi_{uv}\rangle_{AD}$ at each node to obtain maximally entangled states for qudit Bell pairs and achieve an efficient qudit teleportation protocol. Considering this scenario, we discuss the qudit teleportation of $|\Phi_{uv}\rangle_{AD}$, obtained in Eq. (6), after the entanglement swapping. After the purification process of $|\Phi_{uv}\rangle_{AD}$, a maximally entangled qudit Bell pair $|\Phi_{uv}\rangle'_{AD}$ can be obtained, which works as a shared quantum channel between A and D (two nodes).

Now, Alice, who has node A, wishes to teleport an un-

known qudit state $|\phi\rangle = \sum_{j=0}^{d-1} \alpha_j |j\rangle$ to Diana at node D. To proceed, Alice performs a d^2 -outcome joint projective measurement on her qudit A shared with D and the unknown qudit $|\phi\rangle$ to be teleported. She performs a joint projective measurement in a generalized Bell-like basis $\{|\Phi_{uv}\rangle\}$, elements of which can be expressed as

$$|\Phi_{uv}\rangle = \sum_{k=0}^{d-1} \beta_{ku} |k, k \oplus v\rangle, \quad (11)$$

where the symbol “ \oplus ” indicates sum modulo d and the coefficients $\beta_{ku} = \frac{1}{\sqrt{d}} e^{\frac{2\pi i}{d} k \cdot u}$ stand for the extent of entanglement which satisfy the relation $\sum_{k=0}^{d-1} \beta_{ku} \beta_{ku}^* = \delta_{uu'}$. After Alice’s qudit Bell measurement, the combined channel can be written as

$$(|\Phi_{uv}\rangle \langle \Phi_{uv}| \otimes \mathbb{I}_d) |\phi\rangle \langle \phi| \otimes \hat{\rho}_{\text{ch}}, \quad (12)$$

where \mathbb{I}_d is the d dimensional identity operator, $|\phi\rangle \langle \phi|$ shows the density operator of the unknown qudit to be teleported, and $\hat{\rho}_{\text{ch}}$ describes the density operator of the quantum channel shared by Alice and Diana. Alice conveys measurement outcome (u, v) to Diana using an authenticated classical channel. Accordingly, Diana applies a local unitary operation on his qudit given by one out of the d^2 Weyl operators \hat{U}_{uv} [26], defined as

$$\hat{U}_{uv} = \sum_{j=0}^{d-1} \omega_d^{ju} |j\rangle \langle j \oplus v|. \quad (13)$$

After each iteration, the state of Diana’s qudit (up to normalization) can be expressed as

$$\hat{\rho}_{uv} = \hat{U}_{uv} \text{tr}_A \{ (|\Phi_{uv}\rangle \langle \Phi_{uv}| \otimes \mathbb{I}_d) |\phi\rangle \langle \phi| \otimes \hat{\rho}_{\text{ch}} \} \hat{U}_{uv}^\dagger, \quad (14)$$

where tr_A stands for the partial trace on the subsystem of Alice.

While quantum teleportation using quantum entanglement holds great promise, it is highly vulnerable to noise, leading to potential loss of teleported information. However, this challenge can be addressed by leveraging the quantum superposition of different causal orders through a quantum switch [27]. Specifically, if the entanglement is distributed between the sender and receiver using a quantum switch [27], the fidelity of teleportation can be improved even in the presence of noise, enabling a wider range of states to be accurately teleported [28].

III. ENTANGLEMENT SWAPPING AMONG NOISY QUDITS

Thus far, our investigations have focused on pristine quantum systems, carefully shielded from external influences. However, in practical scenarios, quantum systems inevitably engage with their surroundings, encountering a spectrum of disturbances and fluctuations. Among

these, a prominent disturbance is depolarizing noise, also known as white noise. This form of interference transforms the quantum state into a new state by considering a maximally mixed state as \mathbb{I}_d/d . To illustrate, let us examine a scenario involving a noisy biqudit state ρ_{AB}^N , created through the amalgamation of a maximally entangled state ρ_{AB} with white noise:

$$\rho_{AB}^N = \alpha \rho_{AB} + (1 - \alpha) \frac{\mathbb{I}_d \otimes \mathbb{I}_d}{d^2}, \quad (15)$$

where $1 \geq \alpha \geq \frac{-1}{d^2 - 1}$ is the visibility of the system AB, and for simplicity, we choose $\rho_{AB} = |\phi\rangle_{AB} \langle \phi|$ with $|\phi\rangle_{AB} = \sum_{j=0}^{d-1} \frac{1}{\sqrt{d}} |jj\rangle_{AB}$. Equation (15) represents the isotropic form [29] of the system AB. The isotropic systems remain invariant under all unitary transformations of the form $U \otimes U^*$, where the asterisk denotes complex conjugation in a certain basis.

In Bloch representation, the isotropic states can be reformulated as [30]:

$$\rho_{AB}^N = \frac{\mathbb{I}_d \otimes \mathbb{I}_d}{d^2} + \frac{1}{4} \sum_{\mu=1}^{d^2-1} \frac{2\alpha}{d} \lambda_\mu \otimes \lambda_\mu^t, \quad (16)$$

where λ_μ are $d^2 - 1$ generators of $\text{SU}(d)$ group and superscript t represents the transpose operation of a matrix. Now, from Eq. (16), one can construct the Bloch matrix:

$$\tilde{\mathcal{T}} = \begin{pmatrix} c & \vec{O}_1 \\ \vec{O}_2 & T \end{pmatrix}, \quad (17)$$

where c is a scalar number, $T_{\mu\mu} = \text{tr}(\rho_{AB}^N \lambda_\mu \otimes \lambda_\mu^t)$, and \vec{O}_1 and \vec{O}_2 are row and column vectors, respectively, with all entries zero and dimensions $d^2 - 1$. The combo separability criteria [31] tells us that the isotropic states remain entangled if $\|\tilde{\mathcal{T}}\|_{\text{KF}} - 1 > 0$, otherwise, become separable.

Let the particles C and D also be in an isotropic state such that $\rho_{CD}^N = \rho_{AB}^N$. Now the initial state of a four-qudit noisy system is

$$\varrho^N \equiv \rho_{AB}^N \otimes \rho_{CD}^N = (\alpha \rho_{AB} + \beta \mathcal{I}) \otimes (\alpha \rho_{CD} + \beta \mathcal{I}), \quad (18)$$

where $\mathcal{I} = \mathbb{I}_d \otimes \mathbb{I}_d$ and $\beta = (1 - \alpha)/d^2$.

We can generate entanglement between particles A and D by using the entanglement swapping technique for isotropic states of particles A, B and C, D. For this purpose, we make Bell-state measurement on qudits B and C via a complete set of projective operators $|\Psi_{uv}\rangle_{BC} \langle \Psi_{uv}|$, developed from Eq. (5). After Bell measurement on the qudits B and C, qudits A and D which were initially separable, become entangled in the following form:

$$\begin{aligned} \rho_{AD}^N = & \frac{\alpha^2}{d} \sum_{i,j=0}^{d-1} |ii\rangle_{AD} \langle jj| + d^2 \beta^2 \mathcal{I}_{AD} \\ & + \alpha \beta \left(\sum_{j=0}^{d-1} |j\rangle \langle j| \otimes \mathbb{I} + \mathbb{I} \otimes \sum_{j=0}^{d-1} |j\rangle \langle j| \right). \end{aligned} \quad (19)$$

We find d^2 output states ρ_{AD}^N , each with probability $1/d^2$. As both biqudit input states have the same amount of entanglement, all the final states also have an equal amount.

Using now the local unitary operators, one can transform the final noisy entangled states of the qudits A and D, given in Eq. (19), to the following isotropic form:

$$\begin{aligned} \rho_{AD}^{(\mu\nu)} = & \beta \left(\sum_{k=0}^{d-1} e^{-2\pi i \mu k/d} |k\rangle |k \ominus \nu\rangle \right) \\ & \times \left(\sum_{l=0}^{d-1} e^{+2\pi i \mu l/d} \langle l \ominus \nu | \langle l | \right) + (1 - \beta) \frac{\mathbb{I}_{d^2}}{d^2}, \quad (20) \end{aligned}$$

where β is the visibility of the entanglement between qudits A and D. Therefore, for all d^2 quantum states $\rho_{AD}^{(\mu\nu)}$ the average output I-concurrence $C_I^{(av)}(\rho_{AD}^{(\mu\nu)})$ is the same as that of the I-concurrence of each $\rho_{AD}^{(\mu\nu)}$ state.

The I-concurrence [32] of each isotropic state $\rho_{AD}^{(\mu\nu)}$ in Eq. (20) is expressed as

$$C_I(\rho_{AD}^{(\mu\nu)}) = \begin{cases} 0, & F \leq 1/d, \\ \sqrt{\frac{2d}{d-1}}(F - \frac{1}{d}), & 1/d < F \leq 1, \end{cases} \quad (21)$$

where $F = \langle \Psi | \rho_{AD}^{(\mu\nu)} | \Psi \rangle = \beta + \frac{1-\beta}{d^2}$, with $0 \leq F \leq 1$, is the fidelity of $\rho_{AD}^{(\mu\nu)}$ and $|\Psi\rangle = \sum_{k=0}^{d-1} e^{-2\pi i \mu k/d} |k\rangle |k \ominus \nu\rangle$. This fidelity is directly proportional to β , which is the visibility of the swapped entanglement between qudits A and D. It means low noise has participated in the swapping process.

Figure 3 illustrates the relationship between fidelity and I-concurrence for final quantum systems of varying dimensions ($d = 2, 3, 4, 5$). Here, increasing fidelity means the noise of the system gradually decreasing and system approaching to noise free behavior. Thus, higher fidelity corresponds to lower noise and stronger entanglement preservation during the swapping process. The fidelity is plotted along the x -axis, while I-concurrence, an indicator of quantum entanglement, is represented on the y -axis. The curves show how entanglement changes as fidelity varies, with each curve corresponding to a specific system dimension.

At lower dimensions (e.g., $d = 2, 3$), the relationship appears smoother and more inclined, whereas higher dimensions ($d = 4, 5$) exhibit increasingly linear behavior. The blue line shows that we get nonzero I-concurrence even for low fidelity values (around 0.2) in higher-dimensional systems; however, in lower-dimensional systems, the I-concurrence becomes nonzero only at higher fidelities. This observation reflects how dimensionality affects the contribution of β to F , making high-dimensional systems more tolerant to noise and capable of retaining quantum correlations even when the fidelity is relatively low. The figure highlights the significant impact of dimensionality on the interplay between these two key quantum properties, offering insights into the rich structure of entanglement in high-dimensional spaces.

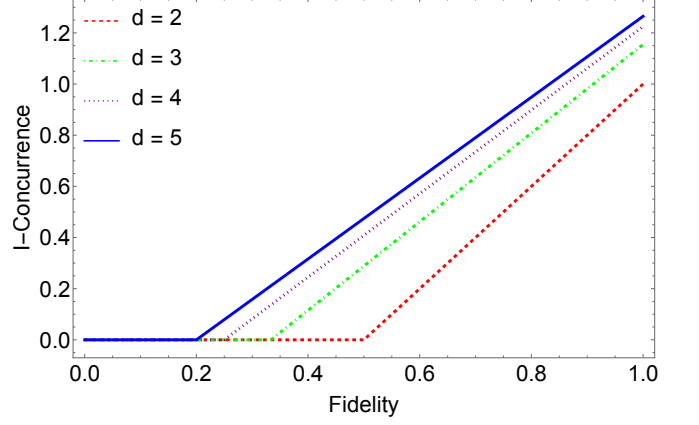


FIG. 3. (Color Online) Variation of I-concurrence with fidelity for quantum systems of dimensions $d = 2, 3, 4, 5$. The curves highlight the dimensional dependence of the entanglement-fidelity relationship, illustrating nonzero I-concurrence with the least fidelity trend as the dimension increases.

The negativity is a measure of quantum entanglement that quantifies the degree of violation of the positive partial transpose (PPT) criterion for separability. To compute the entanglement in terms of negativity, we now consider the partial transpose on subsystem A. After partial transpose of ρ_{AD}^N , we get

$$(\rho_{AD})^\Gamma = \beta (|\Phi\rangle \langle \Phi|)^\Gamma + (1 - \beta) \frac{\mathbb{I}_{d^2}}{d^2}, \quad (22)$$

where Γ represents partial transpose with respect to qudit A and $|\Phi\rangle = \left(\sum_{k=0}^{d-1} e^{-2\pi i \mu k/d} |k\rangle |k \ominus \nu\rangle \right)$. The term $(|\Phi\rangle \langle \Phi|)^\Gamma$ has the eigenvalues $\frac{1}{d}$ and $-\frac{1}{d}$. The first eigenvalue repeats $d(d-1)$ times and the second eigenvalue repeats d times. It means the $(\rho_{AD})^\Gamma$ has eigenvalues $\frac{1-\beta}{d^2} + \frac{\beta}{d}$ (repeats $d(d-1)$ times) and $\frac{1-\beta}{d^2} - \frac{\beta}{d}$ (repeats d times). If $\beta > \frac{1}{d+1}$, then the eigenvalue $\frac{1-\beta}{d^2} - \frac{\beta}{d}$ becomes negative. As negativity is the absolute sum of the negative eigenvalues of $(\rho_{AD})^\Gamma$, so

$$\mathcal{N}(\rho_{AD}) = \max \left(0, \frac{\beta(d+1) - 1}{d} \right). \quad (23)$$

We know that fidelity is given by $F = \beta + \frac{1-\beta}{d^2}$. So, the negativity [23] in terms of fidelity is

$$\mathcal{N}(\rho_{AD}) = \begin{cases} 0, & F \leq \frac{1}{d}, \\ \frac{Fd-1}{d-1}, & \frac{1}{d} < F \leq 1. \end{cases} \quad (24)$$

Figure 4 effectively shows how the relationship between fidelity and negativity depends on the system's dimension. The negativity curve is steep for low dimensions ($d = 2, 3$), indicating that a small increase in fidelity results in a noticeable rise in entanglement. But for dimensions ($d = 4, 5$), the negativity curve flattens. This

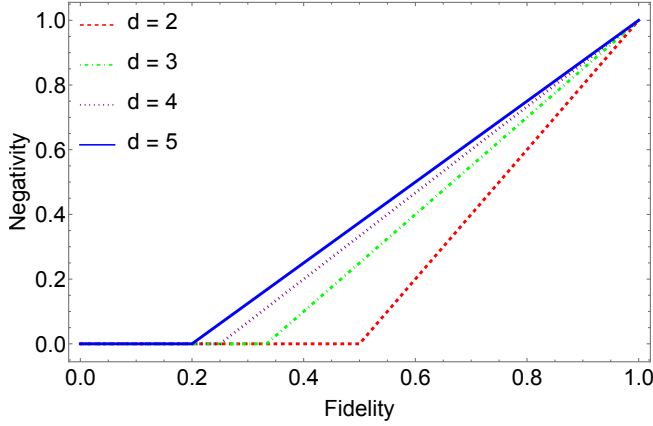


FIG. 4. (Color Online) Relationship between fidelity and negativity for isotropic quantum states across different dimensions ($d = 2, 3, 4, 5$). The curves describe nonzero negativity with the least fidelity trend as the dimension increases. All the curves here converge to $\mathcal{N}(\rho_{AD}) = 1$ for $F = 1$, independent of dimensions.

indicates that achieving high entanglement requires a higher fidelity. It means that as the dimension increases, the relationship between fidelity and negativity becomes progressively less steep, indicating reduced sensitivity of negativity to fidelity at higher dimensions. Negativity increases monotonically with fidelity for each dimension, but approaches a smaller nonzero value of fidelity as dimension d increases.

For each dimension, the negativity starts at zero for $F \leq 1/d$ and begins to rise only when $F > 1/d$. This reflects the separability criterion for isotropic states, where entanglement is only present if $F > 1/d$. For larger d , the negativity increases more gradually as F increases. This is because higher-dimensional systems require higher fidelity to exhibit significant entanglement.

Figures 3 and 4 contrast the dependence of I-concurrence and negativity on fidelity across different dimensions. Figure 4 shows that negativity provides normalized results by remaining strictly within the range $[0, 1]$ for all dimensions. This ensures a consistent and bounded interpretation of entanglement. The curves for negativity exhibit smoother transitions and a more gradual response to changes in fidelity, especially at lower dimensions. In contrast, the I-concurrence in Fig. 3 shows a broader range of values, extending slightly beyond 1 at higher dimensions, indicating that it captures a more detailed or sensitive view of entanglement variations. Additionally, as the dimension increases, I-concurrence curves display a greater slope as compared to the negativity. This contrast emphasizes that while negativity provides a normalized and stable measure of entangle-

ment, I-concurrence offers a more dynamic perspective, particularly in high-dimensional quantum systems. This means that the sensitivity of I-concurrence uncovers intricate relationships between fidelity and entanglement.

IV. CONCLUSION

In this work, we have systematically explored entanglement swapping in qudit-based systems. We also highlighted the advantages of high-dimensional quantum states in facilitating robust and efficient entanglement distribution. Our analysis demonstrates that I-concurrence is a more informative measure of entanglement than negativity in high-dimensional space. Furthermore, we investigated the role of measurement basis selection and initial state configuration in determining the efficiency of the swapping process. Beyond ideal conditions, we extended our study to noisy quantum systems, showing how entanglement swapping can still be effective under realistic conditions. This study paves the way for the next generation of scalable and secure quantum technologies utilizing high-dimensional entanglement.

Khalid Naseer

AUTHOR CONTRIBUTIONS

S. M. Zangi: Writing - original draft, Calculations, Conceptualization, Interpretation of results. **Chitra Shukla:** Writing - original draft, Calculations, Conceptualization, Interpretation of results. **Khalid Naseer:** Writing - original draft, Conceptualization, Investigation. **Saeed Haddadi:** Methodology, Investigation, Writing - review & editing. Thorough checking of the manuscript was done by all authors.

DATA AVAILABILITY

All data that support the findings of this study are included within the article.

COMPETING INTERESTS

The authors declare that they have no competing interests.

- [2] C. H. Bennett, G. Brassard, C. Crépeau, R. Jozsa, A. Peres, and W. K. Wootters, Teleporting an unknown quantum state via dual classical and Einstein-Podolsky-Rosen channels, *Phys. Rev. Lett.* **70**, 1895 (1993).
- [3] A. K. Ekert, Quantum cryptography based on Bell's theorem, *Phys. Rev. Lett.* **67**, 661 (1991).
- [4] C. H. Bennett and S. J. Wiesner, Communication via one-and two-particle operators on Einstein-Podolsky-Rosen states, *Phys. Rev. Lett.* **69**, 2881 (1992).
- [5] M. Hillery, V. Bužek, and A. Berthiaume, Quantum secret sharing, *Phys. Rev. A* **59**, 1829 (1999).
- [6] G.-l. Long, F.-g. Deng, C. Wang, X.-h. Li, K. Wen, and W.-y. Wang, Quantum secure direct communication and deterministic secure quantum communication, *Frontiers of Physics in China* **2**, 251 (2007).
- [7] A. Ney, Separability, locality, and higher dimensions in quantum mechanics, in *Current controversies in philosophy of science* (Routledge, 2020) pp. 75–89.
- [8] M. Żukowski, A. Zeilinger, M. A. Horne, and A. K. Ekert, “Event-ready-detectors” Bell experiment via entanglement swapping, *Phys. Rev. Lett.* **71**, 4287 (1993).
- [9] S. Bose, V. Vedral, and P. L. Knight, Multiparticle generalization of entanglement swapping, *Phys. Rev. A* **57**, 822 (1998).
- [10] J.-W. Pan, D. Bouwmeester, H. Weinfurter, and A. Zeilinger, Experimental entanglement swapping: Entangling photons that never interacted, *Phys. Rev. Lett.* **80**, 3891 (1998).
- [11] S. M. Zangi, C. Shukla, A. U. Rahman, and B. Zheng, Entanglement swapping and swapped entanglement, *Entropy* **25**, 415 (2023).
- [12] W. Dür, H.-J. Briegel, J. I. Cirac, and P. Zoller, Quantum repeaters based on entanglement purification, *Phys. Rev. A* **59**, 169 (1999).
- [13] E. Shchukin and P. van Loock, Optimal entanglement swapping in quantum repeaters, *Phys. Rev. Lett.* **128**, 150502 (2022).
- [14] K. Azuma, S. E. Economou, D. Elkouss, P. Hilaire, L. Jiang, H.-K. Lo, and I. Tzitrin, Quantum repeaters: From quantum networks to the quantum internet, *Rev. Mod. Phys.* **95**, 045006 (2023).
- [15] W. Song, M. Yang, and Z.-L. Cao, Purifying entanglement of noisy two-qubit states via entanglement swapping, *Phys. Rev. A* **89**, 014303 (2014).
- [16] J. A. Bergou, D. Fields, M. Hillery, S. Santra, and V. S. Malinovsky, Average concurrence and entanglement swapping, *Phys. Rev. A* **104**, 022425 (2021).
- [17] V. Karimipour, A. Bahraminasab, and S. Bagherinezhad, Entanglement swapping of generalized cat states and secret sharing, *Phys. Rev. A* **65**, 042320 (2002).
- [18] A. Nourmandipour and M. Tavassoly, Entanglement swapping between dissipative systems, *Phys. Rev. A* **94**, 022339 (2016).
- [19] R.-Z. Cong and S. Xu, Formal bounds of entanglement purification via entanglement swapping, *Phys. Rev. A* **111**, 012409 (2025).
- [20] P. Rungta, V. Bužek, C. M. Caves, M. Hillery, and G. J. Milburn, Universal state inversion and concurrence in arbitrary dimensions, *Phys. Rev. A* **64**, 042315 (2001).
- [21] G. Vidal and R. F. Werner, Computable measure of entanglement, *Phys. Rev. A* **65**, 032314 (2002).
- [22] A. Mair, A. Vaziri, G. Weihs, and A. Zeilinger, Entanglement of the orbital angular momentum states of photons, *Nature* **412**, 313 (2001).
- [23] S. Lee, D. P. Chi, S. D. Oh, and J. Kim, Convex-roof extended negativity as an entanglement measure for bipartite quantum systems, *Phys. Rev. A* **68**, 062304 (2003).
- [24] F. Benabdallah, M. Y. Abd-Rabbou, M. Daoud, and S. Haddadi, Quantum information resources in spin-1 Heisenberg dimer systems, *Quantum Inf. Process.* **24**, 20 (2025).
- [25] J. Miguel-Ramiro and W. Dür, Efficient entanglement purification protocols for d -level systems, *Phys. Rev. A* **98**, 042309 (2018).
- [26] A. Fonseca, High-dimensional quantum teleportation under noisy environments, *Phys. Rev. A* **100**, 062311 (2019).
- [27] I. Dey and N. Marchetti, Quantum teleportation in higher dimension and entanglement distribution via quantum switches, *IET Quantum Communication* **6**, e12122 (2025).
- [28] G. Mylavarampu, S. Ghosh, C. Hens, I. Chakrabarty, and S. Mitra, Teleportation fidelity of quantum repeater networks, *arXiv preprint arXiv:2409.20304* (2025).
- [29] M. Horodecki and P. Horodecki, Reduction criterion of separability and limits for a class of distillation protocols, *Phys. Rev. A* **59**, 4206 (1999).
- [30] M.-C. Yang, J.-L. Li, and C.-F. Qiao, The decompositions of Werner and isotropic states, *Quantum Inf. Process.* **20**, 255 (2021).
- [31] S. Zangi, J.-S. Wu, and C.-F. Qiao, Combo separability criteria and lower bound on concurrence, *J. Phys. A: Math. Theor.* **55**, 025302 (2021).
- [32] P. Rungta and C. M. Caves, Concurrence-based entanglement measures for isotropic states, *Phys. Rev. A* **67**, 012307 (2003).